



ELSEVIER

Contents lists available at ScienceDirect

Ecological Complexity

journal homepage: [www.elsevier.com/locate/ecocom](http://www.elsevier.com/locate/ecocom)

Original research article

## Dimension reduction of multivariate outputs of socio-environmental agent-based models

Ju-Sung Lee<sup>\*,a,b</sup>, Tatiana Filatova<sup>b,c</sup>

<sup>a</sup> Erasmus University Rotterdam, Erasmus School of History, Culture and Communication, Department of Media and Communication, P.O. Box 1738, Rotterdam 3000 DR, The Netherlands

<sup>b</sup> University of Twente, Faculty of Behavioural, Management and Social Sciences, Department of Governance and Technology for Sustainability (CSTM), P.O. Box 217, Enschede 7500 AE, The Netherlands

<sup>c</sup> School of Systems Management and Leadership, Faculty of Engineering and IT, University of Technology Sydney, PO Box 123, Broadway NSW 2007, Australia

## ARTICLE INFO

## Keywords:

Agent-based modeling  
Resilience  
Dimension reduction  
Multidimensional scaling  
Spatial  
Socio-environmental modeling

## ABSTRACT

Often, socio-environmental agent-based models (ABMs) are driven by a host of parameters, and their outputs are similarly multidimensional or vastly high-dimensional. While this complex data and its inter-relationships may be rendered tractable, the task is far from trivial. In this paper, we study the multidimensional outcome space of the socio-environmental, land-use RHEA ABM (Risks and Hedonics in an Empirical Agent-based Land Market), specifically the inter-distances among the outcome measures, and their reducibility using several well-known dimension reduction techniques, variants of multidimensional scalings. In testing the efficacy of several reduction algorithms, we temporally characterize the model's reducibility while exposing changes in behavior across a wide parameter space that can signal sudden or gradual shifts and possible critical transitions. Our findings reveal that the ABM's signature reducibility trends exhibit idiosyncrasies and unexpected non-linearity as well as discontinuities. These non-linearities and discontinuities are indicative of both gradual and sudden shifts, signaling potential propensity to internal perturbations induced by parameter settings. Additionally, we related the outcome space via their inter-distances to the multidimensional input parameter space, effectively assessing outcome "reducibility to model controls". This analysis reveals that the model's sensitivity to parameters is not only temporally dependent, but also can be partitioned by them, some of which suppress variability in this reduction to model controls, raising questions regarding the extent and structure of endogeneity that yields the distinct temporal trends in the relationship between inputs and outputs and their connections to outcome reducibility.

### 1. Introduction

Agent-based models (ABMs) have become increasingly employed in the study of wide array of complex phenomena in the last few decades, including ecological ones (e.g., Brede et al., 2008; Filatova et al., 2013; Grimm and Railsback, 2005; Karsai et al., 2016; Ratzé et al., 2007; Thiele and Grimm, 2010). Within these models, micro-level agents make choices while dynamically interacting with one another and their virtual environments, with varying degrees of spatial and temporal resolution. The decision-making and interactive dynamics are typically theoretically or empirically-grounded but the behaviors and outputs often harbor a range of uncertainty, due to their stochasticity and complexity (Manson et al., 2012). Thus, the agents' behaviors and virtual settings are not fixed but rather guided by a set of input parameters, rules guiding interactions and learning, and endogenously evolving states. Consequently, the complexity of ABMs is exacerbated

not just from its stochasticity, typically accompanying the agents' behaviors and the ABMs trajectories, but by the high dimensional space of parameters and behavioral strategies, all of which set initial conditions as well as shape agents' behaviors, permitting these models to serve as both exploratory and confirmatory tools for analysis. ABMs constitute one class of complex adaptive systems that permit the emergence of complex behavior from heterogeneous agents.

Similarly, complex ABMs tend to produce a large quantity of outputs (or outcomes), that beg for techniques for offering traction in understanding the highly dimensional space of the input parameters and outputs or outcomes. This is especially relevant when modeling socio-environmental system (SES) dynamics, that are known to exhibit non-linearities and at times undergo structural shifts when feedbacks between systems' elements and their macro behavior are changing. Yet, the ABMs exploring this type of phenomena rarely apply quantitative analysis of the output data, in which significant behavior such as systemic shifts are obscured

\* Corresponding author.

E-mail addresses: [lee@eshcc.eur.nl](mailto:lee@eshcc.eur.nl) (J.-S. Lee), [T.Filatova@utwente.nl](mailto:T.Filatova@utwente.nl) (T. Filatova).

<https://doi.org/10.1016/j.ecocom.2018.07.008>

Received 4 September 2017; Received in revised form 3 July 2018; Accepted 13 July 2018

1476-945X/ © 2018 Elsevier B.V. All rights reserved.

through the highly multidimensional data. Dimension reduction methods could be especially useful to detect these shifts – that can signal a system level loss of resilience – by intelligently reducing the complexity of models' output data so that the triggers behind this can be uncovered. The plethora of controllable input parameters as well as the often complex and varying outcomes challenge these goals. While recent literature highlights some of the complexities inherent in and current approaches for ABM output analysis (e.g., Lee et al., 2015), there yet remain many open areas of analytic inquiry. Hence, this paper aims to examine the effectiveness of several approaches in reducing the high dimensional outcome space of an ABM to elicit systemic shifts in model behavior as characterized by structural changes in the relationships between model inputs and outputs.

### 1.1. The problem of reducibility

The abundance of ABM outcomes, some of which are deemed more important than others, challenges researchers to find and apply approaches for rendering the data tractable and interpretable (Turati et al., 2016). A structured accounting of a large set of outcomes can offer insights into the character of the model dynamics. Many methods exist for reducing this high dimensional space for the purposes of, for example, identifying clusters of variables, by often exploiting interdependencies among variables (multi-collinearity) and often producing informative two and three-dimensional visualizations. Reduction algorithms can and have been broadly applied to a wide range of data types containing data points comprising a feature set which may include characteristics and structural positional information. We review some of these later in the paper in Section 1.3.

To address the goal of this paper, we examine a number of approaches that exploit the distance structure as means for understanding aspects of the models' behavior over time, vis-à-vis their reducibility as well as exposing subtle differences among the examined reduction methods. Dimension reduction can be relatively straightforward and visually compelling, allowing for at-a-glance assessment of the data space. While a host of extant approaches effect a reduction in one form or another, we focus on those that attempt to retain the distance structure of the original data. Specifically, we explore a class of dimension reduction methods called *multidimensional scaling* (or MDS), which seeks latent structure within the inter-distances between data points and is often employed for the purposes of information visualization. MDS routines essentially maps a higher dimensional data into a lower dimensional projection and allow for interpretation often through two-dimensional or three-dimensional visualization. The distances between data points in the lower dimensional projection are intended to be as close as possible to the distances in the original dimensions. Alternative dimension reduction techniques exploit additional information surrounding the data points and the relationships to one another, such as nearest neighbors.

In our case, this higher dimensional data comes in the form of multivariate ABM outcome data, each column representative of a key outcome variable and each row linked to a distinct set of ABM input parameters that produced the outcomes. MDS (and other dimension reduction) methods permit a conglomerate treatment of the data space rather than consign the researcher to focus on a small subset, which is often the case for typical (univariate) visualizations and statistical models. However, the reductive capabilities become naturally limited for larger data spaces. The extent and accuracy of the reduction can serve as indicators of the complexity of the ABM's outcomes. That is, less or even increased reducibility, especially if it is sudden, can indicate higher degrees of complexity (e.g., less collinearity) in the ABM behavior and outcomes, while in the presence of some structure and reducibility in those outcomes.<sup>1</sup>

<sup>1</sup> Complete irreducibility however could also indicate a lack of structure or randomness in the model's behavior.

### 1.2. Dimension reduction and resilience

There is a direct linkage between dimension reduction of ABM outcomes and the presence and nature of resilience in an ABM's dynamics. The notion of resilience in environmental ABMs hails from the traditional definitions of ecological/environmental resilience (Folke, 2006). Models designed to study this phenomenon represent a complex adaptive system, and resilience is generically understood to be a system's propensity to achieve a former or new stable state after undergoing internal or external perturbations (Dragicevic, 2016; Walker and Salt, 2006). Environmental, including spatial SES, ABMs addressing resilience are sparse; some recent ones include those that study food web networks (Dragicevic, 2016) and resource consumers (ten Broeke et al., 2017), as well as land use change (e.g., Carabine et al., 2014; Kaplan, 2011; Zia et al., 2016), including the ABM that is used as the example in this paper (Filatova et al., 2015).

In this paper, we argue that the varying extent of reducibility of an ABM's dynamic, multidimensional outcomes permits an inference of resilience or propensity to internal perturbations. While the temporal variance in reducibility can offer a glimpse into when and how a model may meander in the spectrum of simplicity and complexity, sudden shifts in reducibility can be indicative of significant perturbations or structural systemic shifts in the model outcomes. Once a shift has been detected, its trigger can then be further investigated. If the outcomes do not exhibit any dramatic change or remain stable in some fashion after a shift, then the model might be resilient to internal perturbations, as detected by the dimension reduction process itself. We elaborate further on this linkage later in this paper.

### 1.3. Dimension reduction in ecology and ABM studies

MDS techniques appear in various quantitative fields including environmental and ecological studies and, to a lesser extent, agent-based modeling. In ecology, MDS is often labeled as 'ordination'. In studies from the last few decades, we find MDS (and dimension reduction) applications in the study of grassland soil and vegetation (Prentice, 1977), community changes in marine ecology (Clarke, 1993), species' habitat distribution (Guisan and Zimmermann, 2000), forest data (Giraudel and Lek, 2001), environmental threshold detection (Qian et al., 2003), life cycle analyses of wastewater and mussels (Gutierrez et al., 2010), sensitivity analysis of complex watershed models (Sudheer et al., 2011), water reservoirs (Giuliani et al., 2014), tree species distributions (Cunze and Tackenberg, 2015), and spider species and coral assemblages (Hui et al., 2015).

Research comparing MDS techniques have dealt with oceanographic data (Fasham, 1977) and also have been conducted in the general context of ecological studies (Kenkel and Orłóci, 1986). Furthermore, explicit software packages for ecological/environmental analysis that include MDS have been developed (aside from  $\mathbb{R}$  and other packages for statistical language software): for example, PC-ORD (McCune and Mefford, 1999) and PRIMER-E (Clarke and Gorley, 2015).

The use of MDS in ABM output analysis appears less widespread. Some examples of MDS use in ABM analysis include ABMs for ancient urban centers (Jayyousi and Reynolds, 2012), phone center caller profiles (Schroeder and Noy, 2001), political stability (Garces and Alcorn, 2012), and greenhouse gas emissions trading market (Nakada et al., 2011). Murota and Inoue (2014) cursorily mentions MDS' value in ABM analysis while Evans et al. (2013) offers a detailed overview of Sammon's mapping for ABM results at large. MDS has also been applied to networks which can emerge from some ABMs (e.g., Callahan, 2005). Crouser et al. (2012) incorporates MDS visualization in his software for ABM analysis.

However, none so far appear to have comparatively examined reducibility, particularly through MDS, as a way to characterize variations in the complexity of an ABM and its potential to uncover an ABM's capacity for resilience. While studies into ABMs' sensitivities to input

parameters may reveal complex variability in behavior (e.g., [ten Broeke et al., 2016](#)), the goal of this paper is to investigate how latent structures in outcomes may characterize the ABM and how changes in these may signal shifts and the ABM's reactions to those shifts.

## 2. Methodology and data

### 2.1. MDS routines

Several key MDS variants are examined in this paper. These include the classical metric MDS (CMDS), Sammon's mapping (SAM), and variants of non-metric MDS (NMDS).<sup>2</sup> MDS operates on a distance calculation between points in the data sets. Again, the points themselves are multidimensional and can represent two- or three-dimensional spatial coordinates or a data/outcome space of many more dimensions. While there are several options for calculating inter-point distance (e.g., Minkowski's distance), we employ the canonical Euclidean distance. The distance matrix is extracted from a predetermined number of  $n$  data points, each representing a vector of outcomes (or covariates); each cell is calculated as:

$$d_{ij}^* = \sqrt{\sum_{k=1}^m (x_{ik} - x_{jk})^2}$$

where  $x_{ik}$  is value of the  $k$ th outcome variable of the  $i$ th data point (vector) and  $d_{ij}$  is the cell of the  $n \times n$  inter-point distance matrix index by  $i$ th row and  $j$ th column and indicates the calculated distance between the outcome values.

MDS approaches seek a lower dimensional projection while attempting to minimize the error between the original data and the projected data; this error is also called 'stress' or 'strain'. The error function ( $E$ ) for CMDS is:

$$E = \sum_{i < j} (d_{ij}^* - d_{ij})^2$$

where  $d_{ij}^*$  is the distance from the distance matrix of the original data. ([Gower, 1966](#); [Torgerson, 1958](#)). CMDS is also known as Principal Coordinate Analysis (PCoA), Torgerson Scaling, or Torgerson-Gower scaling. An analytical (rather than iterative) solution is obtained through eigen-decomposition and its results are identical to the unscaled scores from Principal Component Analysis (PCA), which also employs an eigen-decomposition when the data is standardized.

Sammon's mapping (SAM) is a non-linear, iterative MDS routine and extends CMDS' error function ([Sammon, 1969](#)):

$$E = \frac{1}{\sum_{i < j} d_{ij}^*} \sum_{i < j} \frac{(d_{ij}^* - d_{ij})^2}{d_{ij}^*}$$

The additional denominator places more focus on the preservation of small distances than CMDS.

Non-metric MDSes also comprise iterative approaches that employ a normalization and a dynamically inferred, monotonically-increasing transformation function  $f$  on the original distances (at each iteration) in order to ensure the distance ranks are maintained. NMDS focuses on congruent ranking of the distances (between the original and project space) and is appropriate for ordinal scale data. Its error function is:

$$E = \frac{\sum_{i < j} (f(d_{ij}^*) - d_{ij})^2}{\sum_{i < j} d_{ij}}$$

The variants of NMDSes examined in this paper are Kruskal's iso-metric MDS (ISO), non-linear monotone MDS under global, local, linear, and hybrid transformation models (NMDS) ([Faith et al., 1987](#); [Minchin,](#)

[1987](#); [Oksanen et al., 2016](#)). The global monotone MDS is most similar to isometric MDS. Local employs a separate  $f$  function for each point. Linear employs a linear regression (rather than a non-linear function) for  $f$ , and hybrid combines local and linear approaches. As each NMDS is a stochastic, iterative process, its performance is subject to vagaries of initial conditions, and often the results of one kind of MDS (particularly CMDS) provides the initial configuration for NMDS. This assists the optimization and voids the "curse of dimensionality", which arises in the case of widely multivariate data.

Various prior studies compare MDS and other dimension reduction techniques. A few examples of these comparisons include several MDS methods along with Isomap ([Kirt and Vainik, 2007](#)), non-linear dimension reduction and solar images ([Banda et al., 2012](#)), gene and protein expression ([Lee et al., 2007](#)), and a comparison between linear (PCA and classical MDS) and graph-based, non-linear techniques ([van der Maaten et al., 2009](#)). However, there has been little comparative exploration of these techniques for ABMs.

### 2.2. Case study: ABM of housing market under environmental hazard risks

In order to understand the irreducibility of ABM behavior, we apply the aforementioned MDS algorithms on output data from an agent-based computational economics model of a spatially explicit empirical housing market, titled "Risks and Hedonics in an Empirical Agent-Based Land Market" (RHEA) ([Filatova, 2015](#)). This ABM simulates a bilateral housing market in an empirical landscape. Buyer agents seek and trade properties with seller agents in a real-life seaside town (Beaufort, South Carolina, USA), where properties are characterized by typical property attributes, and additionally coastal and urban amenities and flood risk. The model is initialized with empirical property prices and characteristics from the years 2000–2004; empirical data is also used to initialize households and their trading rules. The properties have empirical geographic positions and their values are partly dependent on their geographic proximities to local amenities: the coast, centers-of-business (CBDs), parks, and highways. Prices are guided by a hedonic evaluation by a realtor agent, which in turn has been calibrated on a market-based, empirical regression model ([Bin et al., 2008](#)). Further details of the RHEA ABM are provided in [Appendix A](#). To illustrate the utility of DRM methods to characterize the emergence of any potential systemic shifts in the model behavior, we use the output data from the first version of RHEA. The new version of RHEA employs new higher quality datasets, improved price expectation procedure and tests market behavior under various risk perception models ([de Koning et al., 2017](#); [2018](#)).

As is typical of many ABMs, the RHEA model is controlled by a set of input parameters and produces a host of key outcomes ([Appendix B](#)) including agent utility calculations, trade prices broken down by property type categories resulting in the properties' price values, and counts of the agent subpopulations (i.e., buyers, sellers, and realtors). A subset of these input parameters and outcome variables are selected for the MDS analysis in this paper as elaborated in [Section 2.4](#). As for challenges to the model's resilience to external shocks, the RHEA ABM does contain a singular external event, a flood that occurs at a pre-appointed time. However, this parameter is not engaged in this study, in order for us to better understand the model's behavior and the reducibility of its outcomes sans explicit external events. This omission, however, does not shield the model from internal perturbations, as demonstrated in prior work that detected trajectories of evolving states that lead to severe market fluctuations, namely a crash in property prices and in the subpopulation of buyer agents ([Filatova et al., 2015](#)).

### 2.3. Measures

In the analysis, we first focus on the multivariate outcomes of the RHEA ABM and assess their complexity across the life cycle of the model. Through assessing the extent of reducibility afforded by each MDS routine, we also measure and characterize each routine's accuracy.

<sup>2</sup> We employ R's implementations of these algorithms, which appear in different package libraries: `stats`, `MASS` ([Venables and Ripley, 2002](#)), and `vegan` ([Oksanen et al., 2016](#)).

For accuracy metrics, we employ the Pearson product moment correlation coefficient  $r$  (Pearson, 1895),<sup>3</sup> the Kendall rank correlation coefficient  $\tau$  (Kendall, 1938),<sup>4</sup> and root-mean-squared error (RMSE). Each of these is obtained between the upper triangle of the original, symmetric distance matrix ( $\mathbf{d}^*$ ) and the distance matrix calculated from the dimension reduction projection ( $\mathbf{d}$ ).<sup>5</sup> These three metrics account for different qualities of the relationship between distribution of the distances among the original data points and those of the projection.<sup>6</sup>

In the last set of analyses, we examine how the ABM input parameters align with the outcomes as an alternative approach for characterizing the ABM behavior and its reducibility by the relationship between input parameter and outcome dissimilarities. This constitutes a different form of reduction, one in the context of the inputs or controls, and may be labelled as “reduction to model controls”. That is, a model whose outcomes closely mirror the variance in model controls (i.e., input parameters) can be said to be predicted by and reducible to its controls.

#### 2.4. Comparison of MDS routines on empirical RHEA outcomes

We execute and compare the aforementioned multidimensional scaling methods on the ABM outcomes (i.e., output data). The data consists of outcomes from 1000 simulation instances (or runs), each driven by 1000 distinct sets of 11 input parameters. These parameters initially set and drive the model’s mechanisms and have been of research interest in past work on the model (Filatova, 2015; Filatova et al., 2015). Thus, each of the 1000 input parameter sets controls a distinct simulation run that is run for 100 time steps, a temporal horizon long enough to allow for variability in this ABM’s outcomes.

As the RHEA model simulates an empirically-informed real estate/housing market of an empirical geographic region under flood risk (Filatova, 2015), the standard time horizon employed has been 30 years, representing the common mortgage for house buyers. Each time step (or ‘tick’) represents 6 months, which was derived via calibration of the model in previous work. Thus, the typical number of time steps is 60. For this paper, we extend the time horizon beyond 60 steps to 100, in order to acquire a more robust understanding of the model in the context of its outcome reducibility. The 11 input parameters and 19 outcome variables that we assess span important model inputs and outputs and are described further in Appendix B. As with the input parameters, the outcome variables selection is guided by their prior research importance and interest (Filatova, 2015; Filatova et al., 2015; 2011) to the understanding of a housing market under flood risk. These two sets of variables then define an 11-dimensional input and a 19-dimensional output space. The input parameters are uniformly sampled from a 11-dimensional hypercube; the ranges of each dimension are

described in Table B.2 in Appendix B. The uniform distribution is employed for unbiased sampling as a diffuse prior given that we desire to explore a dispersed range of parameterizations, that are partly constrained by calibrations undertaken in previous work on this model.

### 3. Results

We first conduct a diagnostic investigation using correlations to acquire some preliminary understanding of how the outcomes are related throughout the model runs. Fig. 1 displays the inter-variable correlations (Pearson  $r$ ) or collinearities among each of the input and outcome variable sets, at the starting and ending time steps. That is, each colored cell represents pair-wise correlations over all 1000 simulation runs. There ought not to be any visible structure in Fig. 1a, as the input parameters were randomly sampled and also remain static through each model’s run as they only set the initial controls to the ABM. Hence, the heat map is dominated by dark blue (i.e., no or little correlation). As for the model’s outcomes, they are highly correlated in the initial time step of the model as the simulation has not had sufficient time for the outcomes to diverge from the initial conditions. This is largely due to the model outcomes’ aligning closely with the initial empirical housing prices, and the housing market has not yet had a chance to fluctuate as transactions among the agents have barely begun to occur. (Fig. 1b). We naturally expect the model behavior and outcomes to deviate from these initial conditions in the subsequent time steps. Specifically, the feedbacks between input parameters, including valuation of particular spatial environmental attributes by agents with heterogeneous incomes and preferences, evolve signaling either an incremental or structural change at the aggregated level of this SES. The latter – when identified by means of DRM techniques – indicates a presence of systemic change in the model behavior.

By the end of the pre-specified time horizon Fig. 1c, we observe a few clusters of variables that are moderately to highly correlated (collinear). This diagnostic analysis then signals potential reducibility in the outcomes, but not all of them. The collinearities indicate that, at least at the end of the pre-specified time horizon, some outcomes conform despite their differing ranges and the wide range of random input parameters. Specifically, the outcomes that appear collinear represent, in separate clusters, the prices of different kinds of properties and different measures of the seller population. These two distinct sets raise our expectations that the chosen model outcomes will exhibit some reducibility, at least by time step 100, driven by housing property price and seller population indicators. Given that artifacts in the outcomes could bias these correlations and also become problematic for dimension reduction, it behoves us to further prepare the outcomes data for the reduction.

In preparing the data for the dimension reduction analysis, we perform several, necessary steps. First, each variable is standardized allowing them to be aggregated in the distance computations,<sup>7</sup> thus eliminating the extreme weighting incurred by several outcome variables that have large absolute magnitudes. Similarly, we eliminate highly influential outliers: those cases having any variables that lie beyond 4 standard deviations:  $\sigma > 4$ . Also, due to the difficulties for some of the iterative MDS algorithms in handling closely occurring points in the outcome distance matrix, we eliminate these near duplicates. That is, for pairs of points within a standardized  $\epsilon < 0.1$ , only one is kept in the analysis. Near duplicates occur only in the initial steps of the model; that is, counts of 9, 2, and 1 near duplicates are respectively removed from time steps 1, 2, and 3.<sup>8</sup>

<sup>7</sup> In statistical standardization, each variable is 1) centered by its mean and then 2) scaled (divided) by its standard deviation.

<sup>8</sup> The average count of outcome sets removed across all time periods due to near duplicates and outliers in any of the outcome variable is 27.1 (out of the 1000 data points per time step) ( $\sigma = 5.9$ ). There is a slightly increasing (and statistically significant) trend of 0.10 outliers per time step. Thus, the size of the correlated vectors varies from one time period to the next, and lie in the interval [958,994].

<sup>3</sup> The Pearson product-moment correlation coefficient  $r$  is calculated as:

$$r = \frac{\sum_{i=1}^n (x_i - \bar{x})(y_i - \bar{y})}{\sqrt{\sum_{i=1}^n (x_i - \bar{x})^2} \sqrt{\sum_{i=1}^n (y_i - \bar{y})^2}}$$

<sup>4</sup> The Kendall  $\tau$  calculated is as follows:

$$\tau = \frac{(\text{number of concordant pairs}) - (\text{number of discordant pairs})}{\frac{1}{2}n(n-1)}$$

where number of concordant pairs =  $\sum_{j>i} I\{(x_i > x_j \ \& \ y_i > y_j) \text{ or } (x_i < x_j \ \& \ y_i < y_j)\}$  and number of discordant pairs =  $\sum_{j>i} I\{(x_i > x_j \ \& \ y_i < y_j) \text{ or } (x_i < x_j \ \& \ y_i > y_j)\}$

<sup>5</sup> RMSE is:

$$\text{RMSE} = \sqrt{\frac{\sum_{i=1}^n (x_i - y_i)^2}{n}}$$

where  $x$  and  $y$  are vectors of length  $n$ .

<sup>6</sup> While Pearson  $r$  is sensitive to outliers, it can be superior to  $\tau$  in under Gaussian distributed data (Chok, 2008).

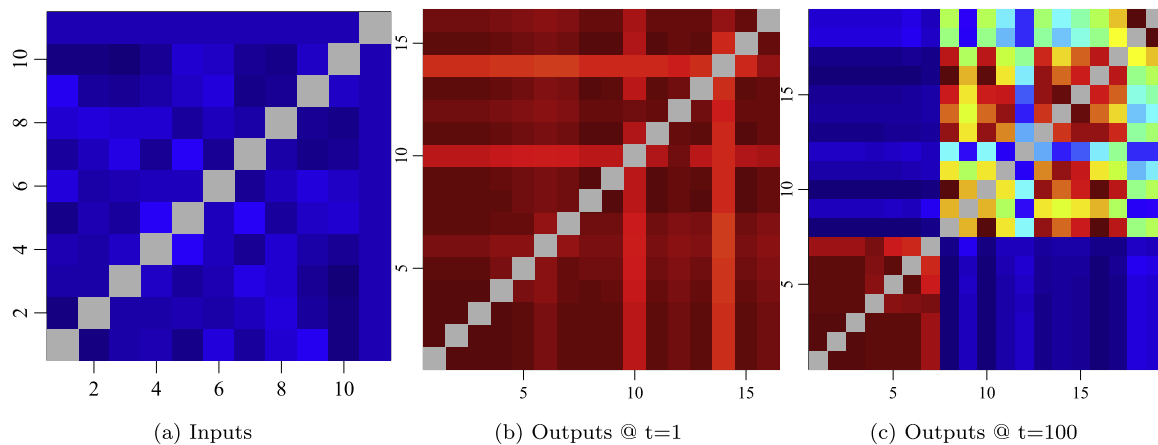


**Fig. 1.** Pearson correlation among variables. The **dark blue** denotes the minimum correlation of  $-0.12$  and **dark red** indicates a maximum correlation of  $1.0$ . (For interpretation of the references to color in this figure legend, the reader is referred to the web version of this article.)

Furthermore, the iterative MDS routines (SAM and NMDSEs) require an initial starting configuration of the projected space. Preliminary analysis revealed that using the CMDS results for the initial configuration consistently produces the most accurate results.

### 3.1. Parameterization of MDS routines

We now focus on the data reduction itself, specifically to a projection of two dimensions; the choice of two dimensions is partly motivated by the need to often conveniently visualize MDS results. Our future work on this subject will include testing of extended dimensional projections, and we discuss the implications of extended dimensions in the conclusion of this paper. First, we discuss the parameterizations we employ for the MDS routines themselves (i.e., not of the RHEA model). Different parameterizations were examined in order to observe the impacts of the algorithms on the extent of reduction that could be obtained.

For the iterative non-metric procedures, we examine the effects of stringent and less stringent (or “fast”) stopping/convergence criteria; the former renders the speed of the algorithms to be slower yet more accurate.

Algorithm	Fast		Slow/Accurate	
	Max. Iter.	Conv. Crit.	Max. Iter.	Conv. Crit.
Sammon	100	$10^{-4}$	10,000	$10^{-10}$
SAM				
Kruskal	50	$10^{-3}$	10,000	$10^{-10}$
ISO				
monotone	200	$\{10^{-4}, 10^{-7}, 10^{-5}\}$	10,000	$\{10^{-10}, 10^{-10}, 10^{-10}\}$

The NMDS employs three distinct convergence criteria/parameters, hence the set of three values. These are 1) the stress, 2) the scale factor of the gradient, and 3) the stress ratio, computed as  $1 - \text{the displayed value}$  (e.g.,  $1 - 10^{-5}$  or  $0.99999$ ).

We employ the canonical Euclidean distance among outcome vectors for inter-outcome distance at each time step:<sup>9</sup>

$$d_{ijt}^* = \sqrt{\sum (\mathbf{x}_{it} - \mathbf{x}_{jt})^2}$$

where  $\mathbf{x}_{it}$  is the vector of 19 outcomes born of the  $i$ th sampled input parameter set at time step  $t$  (with  $j$  similarly treated); hence,  $d_{ijt}^*$  is the

<sup>9</sup>A brief investigation into Minkowski’s distance (a generalization of Euclidean distance) reveals that Euclidean distance is more appropriate for these analyses.

Euclidean distance (a scalar) between vector of 19 outcomes produced by parameter sets  $i$  and  $j$  (of the 1000 generated simulation outcome sets) at time  $t$ , and so  $\mathbf{d}$  denotes the full, symmetric distance matrix among outcome sets at time  $t$ . A matrix of largely low distances would indicate that the uniformly sampled input parameters produce similar outcomes and indicate the outcomes’ resistance to varied distances in input parameters, while high distances would indicate great heterogeneity in the model’s behavior and sensitivity to the input parameters.

Each application of an MDS algorithm produces a set of coordinates in two-dimensions. We then compute the Euclidean distance matrix of this set to compare against the distances among the original outcomes. Again, we consider only the upper triangle of the symmetric distance matrices in calculating the accuracy (correlation and RMSE) metrics. Specifically, we obtain two vectors of distances, one from the original and another from a target matrix, e.g.,  $\Delta^u(\mathbf{d}^{\text{original}}) = (d_{12}, d_{13}, \dots, d_{ki})$  where  $k > l$  and each indexes the original outcomes of a particular input parameter set and  $\Delta^u(\dots)$  indicates extraction of the upper triangle. Then,  $\Delta^u(\mathbf{d}^{\text{reduced}})$  represents the upper triangle of the distance matrix calculated from the two dimensional projection from the application of an MDS routine.

### 3.2. Implications of shifts in reducibility

Any temporal change in the quality of dimension reduction of outcomes (as detected through the aforementioned correlation metrics) has a specific implication on variation of the outcomes. That is, a sudden shift in reducibility across time would indicate the sudden departure of a subset of outcomes from the trend established by other outcomes and/or by similar outcomes of other input parameter sets, a structural shift. To illustrate this point, we imagine that there are only four outcome variables: X, Y, Z, and A. Across all 1000 random input parameter sets, let us say that outcomes X and Y are perfectly correlated, and Z and A are also perfectly correlated (at some time  $t$ ). However, X/Y and Z/A need not be correlated to one another. A dimension reduction to two dimensions would result in distances that perfectly align with X/Y and Z/A as these already span a simple 2-dimensional space. However, if for some subset of those 1000 simulation runs, any of those outcome variables departs significantly, due to internal or external perturbations in the model, the four variables would no longer be perfectly reducible to two dimensions. Thus, a sudden change in the correlation between the original and reduced distance matrices would indicate a sudden shift in some of the outcomes for some of model runs. A shift does not necessarily have to manifest as a loss in reducibility as it can also confer greater reducibility (i.e., higher inter-outcome correlations). Whether or not such shifts are detected and how the model reacts to such shifts can be indicative of its resilience to some internal or external

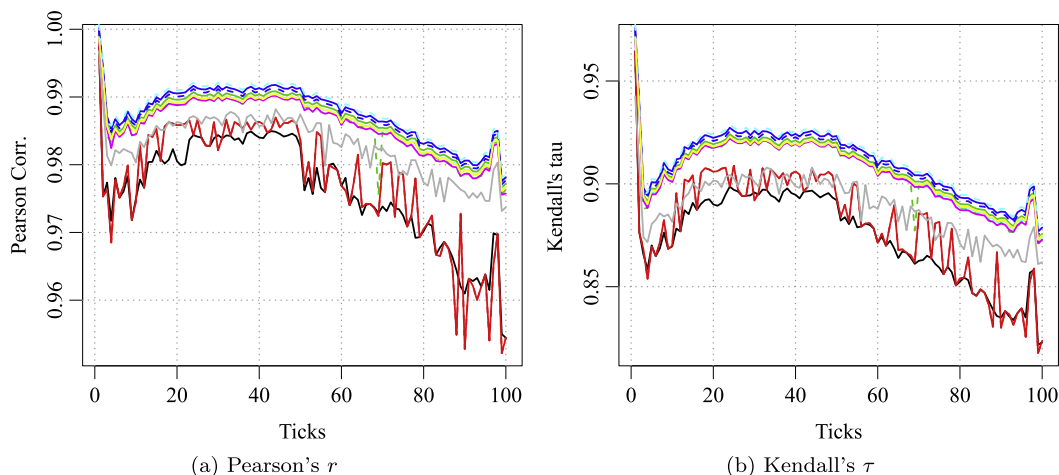


**Fig. 2.** Reducibility measured by correlations. The colors indicate classical metric MDS, Sammon mapping, Kruskal's non-metric MDS, and variants of the monotone MDS: global w/rescaling, global w/o re-scaling, local, linear, hybrid. The dashed line indicates the less rigorous, 'fast' stopping criteria. Overlaid lines of the upper curves are slightly offset in order to render them visible in the plot. (For interpretation of the references to color in this figure legend, the reader is referred to the web version of this article.)

perturbations.

### 3.3. Reducibility of model outcomes

Next, in order to assess the reducibility of model outcomes, we compare the actual distance matrix of outcomes (per time step) to the reduced distance matrix using the correlation and RMSE metrics outlined earlier in the method section. This comparison confers the accuracy of the tested MDS algorithms using correlations, as discussed in Section 2.3, as well as a characterization of the outcome reducibility across time. In Fig. 2, the Pearson's  $r$  and Kendall's  $\tau$  between the outcome data and each of the MDS routines, applied on (the upper triangles of) the distance matrices of the outcome data, are displayed. The functional notation for  $r$  at time step  $t$  is then  $r(\Delta^u(\mathbf{d}_t^{\text{original}}), \Delta^u(\mathbf{d}_t^{\text{reduced}}))$  and similarly for  $\tau$ .

First, we observe the overall correlations between the distances in the original outcome space and the projected 2-dimensional space to be surprisingly quite high, between 0.95 and 1.00 for  $r$  and 0.80 and 0.96 for  $\tau$ . This is partly due to the clusters of collinear outcomes observed in Fig. 1. Also,  $r$  and  $\tau$  appear to exhibit similar patterns across time, with  $\tau$  naturally having lower correlation values.

We also observe that the NMDS and ISO MDS routines are consistently superior to CMDS and SAM. In fact, with the exception of the "fast" convergence criterion in ISO (dashed green), the former are nearly identical.<sup>10</sup> Also, Sammon's mapping appears to exhibit far more variance than CMDS as observed by its greater amplitudes in its oscillations across time. While it can offer on average higher relative accuracy than CMDS, its effectiveness appears (at least from these figures) qualified, especially considering the non-metric routines offer superior accuracy. Still, the hybrid condition (gray) is consistently less accurate than the other NMDS routines. While the hybrid condition is contingent on an exogenous criterion for determining when local or linear approaches engage for a given distance, it is somewhat surprising that it underperforms both of those approaches.

The dominant curvature exhibited by all of the MDS routines can be described as an initial, sudden but transient departure from lower dimensional conditions to gradual resurgence of reducibility, followed by an increase of irreducibility and complexity. As mentioned earlier for Fig. 1a, the initially high correlations at the first time step is indicative of the latent lower dimensional structure occupied by the 19 outcomes. The model initiates from a quiescent state from which further activity is

borne, and market mechanisms in the model are not extremely volatile at that stage. Furthermore, several count outcomes retain a value of 0 across all parametric conditions in the initial step.

The model then quickly diverges from this homogeneous state as subsequent activity renders the outcome space to become more complex and less reducible. Thus, by time step 4, the reducibility of distance structure reach its first nadir. At this point, the outcomes have suddenly deviated from another (a structural shift), as cumulative stochasticity impacts the model. Thus, this apparent initial altered dynamics is trivial and expected behavior. After this point, the behavior of the system, as characterized by reducibility in the outcomes, gradually begins to become lower-dimensional, indicated by the resurging correlations.

With the exception of the scaled monotone MDS, all trajectories reach a peak (or temporary plateau) of reducibility between steps 25 and 45, after which the outcomes diverge again and in fact continue to do so. Internal perturbations, dissimilar to the sudden ones observed in the initial stages of the model, occur resulting in outcomes to gradually deviate from the others rendering the model less reducible. Recall that outcome sets that included severely outlying values are removed from this analysis; thus, the divergent trend is not caused by any outliers. Further, the CMDS and SAM routines appear to signal the downtrend given the noticeable dip in reducibility, particularly in CMDS, just prior to the downtrend. Given that a trajectory of worsening reducibility follows the dip, we can say that the model (in some of the parameterizations) has become susceptible to that emergent shift (i.e., the aforementioned dip), a vulnerability that had been building up endogenously in the model.

Near the end of the pre-specified time horizon (i.e., near time step 100), there is a minor resurgence in reducibility as the correlations briefly climb, peak, but then re-conforms to the curvilinear trend. Thus, for a brief moment, a portion of the outcomes suddenly conform to the inputs. This shift in reducibility signifies a different kind of loss to resilience, one in the context of the pattern of decreasing reducibility in this phase of the model and emergent from an unknown subset of the input parameter sets in combination with internal model dynamics.

As mentioned the method section, we also assess the reducibility accuracy using the root mean-squared error (RMSE). In Fig. 3a, the original distance matrices are compared to the distance matrices from each MDS projection, at each time step with this measure. The RMSE is largely proportionally identical to Euclidean distance and lower RMSE values, unlike the correlations, indicate greater congruence between the original and projected distance matrices, hence, reducibility of the

<sup>10</sup> ISO 'fast' experiences a drop in the correlation near time step 70.

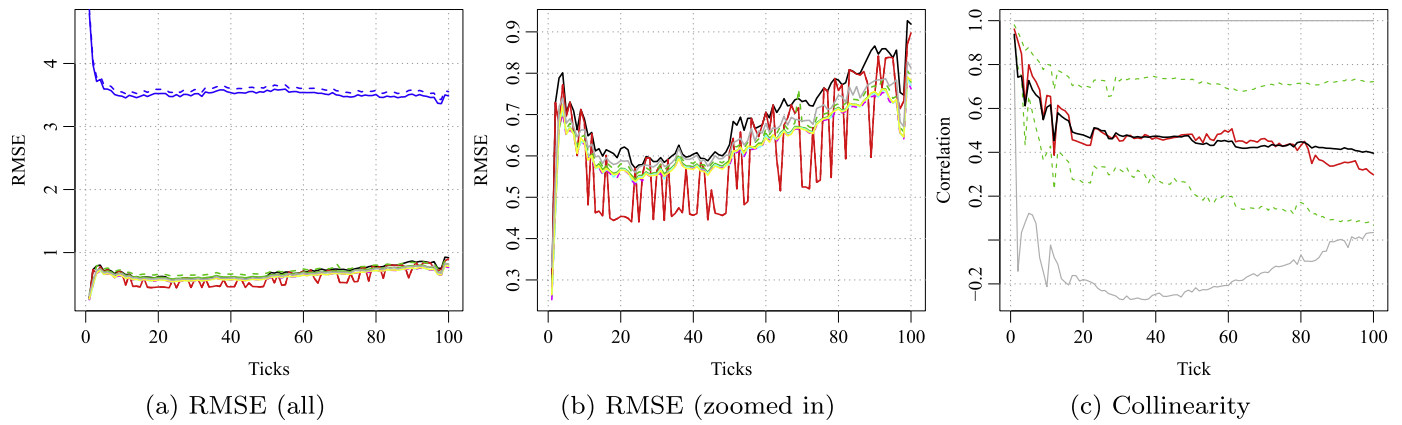


**Fig. 3.** Reducibility measured by RMSE and collinearity. *In the right plot, the mean, median, 1st and 3rd quartiles, and the lower and upper bounds are plotted.* (For interpretation of the references to color in this figure legend, the reader is referred to the web version of this article.)

model outcomes.<sup>11</sup>

The graph colors in the first two subplots correspond to those in Fig. 2. The most salient observation is that the raw RMSE error from the scaled monotone MDS (blue) renders it to be an inaccurate option. This is not entirely surprising given that the projection is rescaled to the root mean square for each step of the iteration, thus destroying the span of the original distance space. Despite this pessimistic finding, the rescaled monotone actually produces noticeably better correlations under different initial configuration conditions (analysis not included), while the unscaled version is only slightly superior.

Naturally, the reduction patterns offered by RMSE for the other MDS routines (Fig. 3b) are consistently the converse of the correlation patterns, as RMSEs represent dissimilarity while  $r$  and  $\tau$  represent similarity: the model’s reducibility initially drastically falls, rises again only to continue to become less reducible. Also, we notice that Sammon’s mapping is often superior to the other metric and non-metric routines, while its correlations were only occasionally superior to classical MDS and inferior to the other non-metric routines. This incongruity renders the researcher’s selection of MDS routine to be dependent on the objective: correlation or error minimization. If our goal is to accurately depict the system’s behavior according to RMSE, we would opt for Sammon’s mapping. If either of the correlations,  $r$  or  $\tau$ , has higher importance, then we would select one of the other non-metric routines. Similarly, CMDS’s performance is only slightly worse (relatively) here than it is under the correlation metrics, making it a viable candidate for use if raw accuracy (i.e., RMSE) is more important than correlation.

As an additional diagnostic, we revisit the relationship among outcomes (shown earlier in Fig. 1) but here across all time steps. As with the earlier figure, we focus on the correlation ( $r$ ), but now report on its various descriptive statistics. Fig. 3c displays the mean, median, 1st and 3rd quartiles, the minima and maxima statistics of the inter-correlations ( $r$ ) among the outcomes themselves. These statistics apply over all the inter-correlations among the outcomes, i.e., the upper triangle of the values underlying Fig. 1c, but across all time steps.

Surprisingly, most of the patterns do not fit those of the reducibility measures. While the mean and median collinearities are initially high (expected), they gradually drop. If one were to describe a dynamic system solely based on the pattern of collinearity, one would infer that the system monotonically increases in its complexity and higher dimensionality, rather than the non-linear patterns observed in Figs. 2 and 3b that exhibit multiple local minima and maxima. However, we observe that the minima of the collinearities (lower correlation bounds, beyond the initial steps) bear some resemblance to the RMSEs. It

remains possible that the descriptive statistics of the collinearities has a functional relationship to the MDS and RMSE patterns, one that is driven by the minimum inter-outcome correlation at each time step.

### 3.4. Reducibility to model controls

While distance measurements (among outcome sets) when reduced through dimension reduction reveal latent structure and varying levels of reducibility across time, they can also reveal subtle relationships between the simulation input parameters (or model controls) and the outcomes. Here, we explore the extent to which the distances between the input parameter sets themselves, which we re-iterate are sampled randomly, relate to the distances among their resultant outcome sets. To illustrate this relationship, consider the case when the correlation between the distances among the parameters and the distances among the outcomes (at some given time  $t$ ) is very high, say 0.80. This would occur if differences (i.e., distances) between pairs of input parameter sets (from the set of 1000 input parameter sets) correlate highly with differences among their associated outcome sets (at some given time  $t$ ). Such a high correlation indicates that the model outcomes are driven by, and reducible to, the varied distances in the input parameters and signals some extent of predictability and adherence of outcomes to input parameters. Thus, investigation in this relationship can reveal a different kind of complexity and reducibility, one that is subject to model controls.

For this analysis, we require a distance matrix of the static input parameters  $\mathbf{d}^{\text{input}}$  where ‘input’ here denotes input parameters. Thus, each cell of this matrix ( $d_{ij}^{\text{input}}$ ) represents the distances between input parameter sets  $i$  and  $j$  (out of the 1000 uniformly sampled, randomly generated input parameters set used in the earlier MDS analyses of this paper). We can easily correlate the upper triangles of the symmetric distance matrices:  $r(\Delta^{\text{u}}(\mathbf{d}^{\text{input}}), \Delta^{\text{u}}(\mathbf{d}^{\text{original}}))$  where  $r$  is the Pearson correlation (substitutable with Kendall’s  $\tau$ ) and again  $\Delta^{\text{u}}(\dots)$  extracts the upper triangle of a matrix. Here, correlations are computed between the input parameters and both the (a) data with outliers (called ‘full’ data) and (b) input and outcome sets harboring outliers (at a given time step) removed (here, labeled ‘nominal’).<sup>12</sup>

Furthermore, for this exploration, we also explicitly distinguish outputs induced by variations in a key experimental condition. That is, we conduct this analysis on two partitions of our initial set of input parameters based on a key parameter of realtor agent adaptivity (a binary parameter). This parameter controls the adaptivity of the hedonic function (i.e. regression model for assessing property value) that the realtor agents, who broker the housing transactions, employ in setting prices. This partitioning of analysis is motivated by our

<sup>11</sup> We say “largely” due to the omission of outliers and near duplicates.

<sup>12</sup> The removal of outliers is described in earlier in the result section.

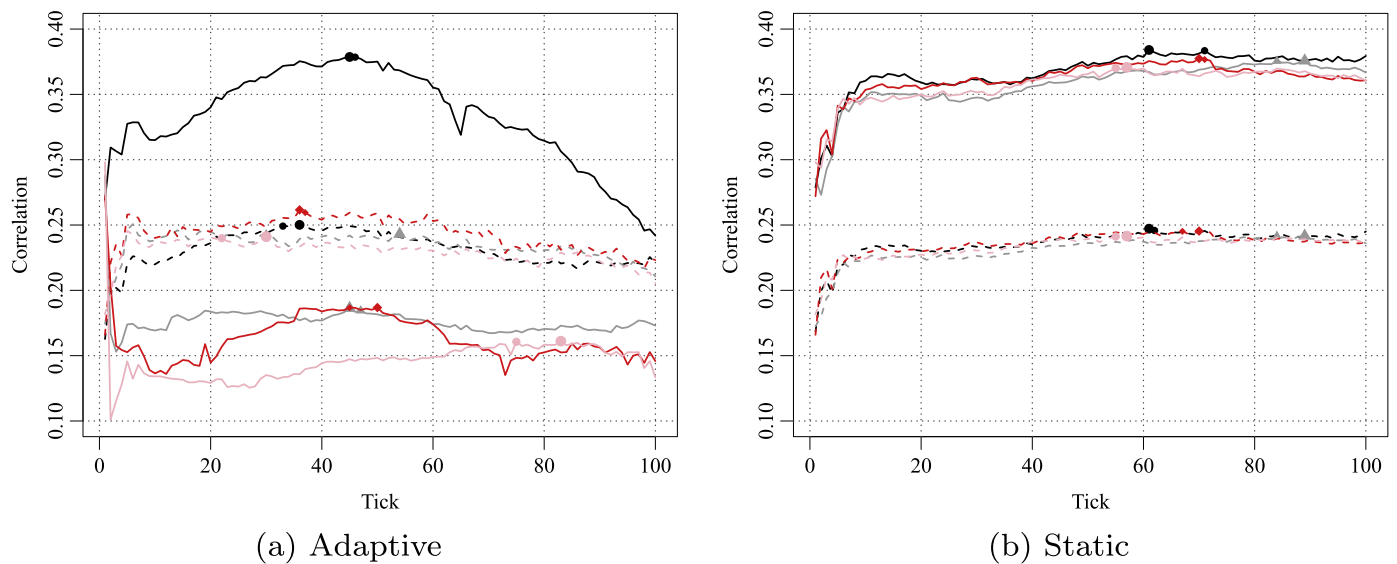


**Fig. 4.** Reducibility to model controls by conditions. *The solid curves indicate Pearson's  $r$  correlation and the dashed, Kendall's  $\tau$ . The large dot denotes the maximum of each curve, while the smaller dot, the sub-maximum. The black and red curves respectively denote the nominal (outliers removed) and full data (including outliers). The lighter color tones (gray and pink) indicate those runs in which the initial seeds for the model runs were identical. (For interpretation of the references to color in this figure legend, the reader is referred to the web version of this article.)*

suspicion and prior observations that the model's behavior differs substantially when this agent's adaptivity parameter is engaged ('Adaptive') compared to when it is not engaged ('Static').

The correlations for both  $r$  and  $\tau$  vary between 0.10 and 0.37 and are all statistically significant ( $p < .001$ ); the significance ( $p$ ) of each correlation is determined via a permutation test (the Mantel test (Mantel, 1967)), which generates a null hypothesis that controls for matrix auto-correlation. This lower range of correlations (as compared to those from the MDSes) indicates the model outcomes' being less reducible to model controls than their own reducibility. The maxima indicate the time points at which the distribution in the distances between the input variables (constant) and the output variables are most congruent.

The features in Fig. 4a, particularly the solid red curve (the nominal data), partly mirror those of the correlations (Fig. 2). Namely, there is a striking shift in similarity at the onset of the model runs, followed by a gradual rise to a peak within ticks 25–45 – indicating the time range at which the input variables are most predictive of the output – and ultimately a decline that falls below any of the initial levels. While much of the curvilinear trend particularly with the nominal data mirrors the trends observed for the outcome-only reduction earlier in the paper, the interpretation of the pattern is not the same here. Here, we infer that when the correlation is relatively high, the distribution of model outcomes (specifically, inter-outcome distances) are aligned with the distribution of the input parameters. Hence, the input parameter distances are most predictive (for the 'nominal' filtered data) not at the starting stages, but later on when the model has had a chance to mature.

In contrast, the static hedonic condition yields a much more tempered pattern noted by general flatness, the outcomes of which yet retain a similarity as high as the outcomes from most similar adaptive time step. That is, the model rises quickly to its highest relative levels and more-or-less remains at that level. From this, we learn that dynamism infused into a key decision-making element (i.e., adaptivity in the hedonic regression) greatly impacts variations in the model's reducibility to controls, specifically inducing behavioral regimes in which there is less association to the variations in the controls, as indicated by the lower correlations in the Adaptivity condition compared to the Static condition.

Finally, another idiosyncrasy is detected near time step 65 for nominal data (solid black curve) in which there is a sudden, but

recovered, drop in the outcomes' correlation to model controls. This and the previously observed idiosyncratic shift in reducibility near time step 100 (in Fig. 2) do constitute latent divergent trajectories as the dominant trends toward less reducibility seems to resume in both cases and their resumption could signal a different kind of resilience; that is, in both cases the outcomes surge in their alignment to one another and to model controls, but this is defeated by the continuing divergent trajectories of some of the simulation runs. What we observe here is similar to earlier, a sudden departure in the outcome behavior: a structural shift in the data born of one or more of the controls, but one that is not detected from the MDS.

#### 4. Conclusion

This paper investigated ABM outcome reducibility to characterize varying levels of complexity in its outcomes and their connection or reducibility to the model's inputs or controls. As such, we examine the effectiveness of several approaches in reducing the high dimensional outcome space of a SES ABM to elicit endogenous systemic shifts in model behavior as characterized by structural changes in the relationships among the model outcomes and between the outcomes and inputs. In order to do so, we first applied several dimension reduction (MDS) algorithms to the outcomes of the socio-environmental RHEA ABM and also compared the MDS' results (i.e., distances born of their two-dimensional projections) to the distance structure of the model controls. Consequently, we exposed the extent and timing of reducibility to both a lower dimensional space and to the varied distances in the randomly sampled input parameters. Simultaneously, these results can reveal when and how the model exhibits higher levels of complexity, indicated by outcome regimes of lesser reducibility or lesser association to model controls. In the case of the outcome data of this paper, complete irreducibility – that would be detected through the complete lack of inter-outcome correlation – is not manifest. Thus, one can argue that the model's behavior remains within the spectrum of randomness and perfect deterministic predictability. Still, the focus on outcomes cannot reveal the complexity (or simplicity) of the model mechanisms themselves, a limitation of this approach.

The trajectory of reducibility across the model's time horizon as measured by the three association measures (i.e., two correlations measures and RMSE) offers a characterization of the behavior of RHEA



ABM. That trajectory exhibits several local extrema and describes the model's global behavior as well as raising questions as to the exact drivers of the curve. This trajectory broadly identifies a region of behavior, in which the model outcomes initially are trivially reducible (high correlation) but then quickly becomes less so until reaching a local minimum for reducibility. Thus, the model's stochastic mechanisms rendered the outcomes resilient to any and all of the initial empirical conditions and the breadth of the tested input parameter sets, a finding that is largely expected given the model's mechanisms. Then, dynamics of the model evolved, gradually increasing collinearity hence correlations in the MDS, among the outcomes only to diverge again further down the time horizon, becoming increasingly less reducible. This reduction in reducibility likely coincides with a critical transition within a subset of the simulation runs, as indicated by the sudden decrease in the correlation for two of the MDS routines: SAM and CMDS. In fact, such a decrease following a near plateau in the reducibility then followed by further gradual decrease may indicate a critical threshold and serve as an early-warning signal for a critical transition, the detection of which has been recognized to be desirable yet difficult to achieve (Lade and Gross, 2012; Scheffer et al., 2009; SPARCS, 2018).

The observed trajectory is then interrupted briefly by an up-spike near the end of the measured run cycle, which indicates an additional structural shift in some of the outcomes, but towards more alignment rather than the trend of divergence in the outcomes. This however is dominated by the increasing divergence in outcomes as reducibility continues to decrease. We can consider the overall curvature and our interpretation to be precise given that it appears with only minor variations across all three metrics and all eight MDS routines. These variations also highlight the complexity of ABM and the outcome space. Otherwise, the curves would appear less offset from one another and smoother. That is, the fact that the MDS routines did not perform identically, despite the similar temporal pattern, offers another facet of the model's complexity. However, the trajectory itself is not overly complex, and its discontinuity may be defined by two separate functions, suggesting an approach to typifying this particular model's outcome space, as portrayed by MDS and the metrics, that might also be applied to outcomes of other ABMs.

One point of note is that reducibility is rather high as the correlations between the original and the reduced distance matrices are above 0.85 for both correlation measures across all time points. The diagnostics earlier in the paper offers indication that two clusters of outcome variables (regarding property prices and the sellers market) may primarily drive the overall strong reduction. Thus, one implication of this finding is that to better understand the model's behavior under a wide array of input parameters, these variable sets can be aggregated in order to uncover a different layer of reducibility, albeit a less precise one as the non-correlative variables would then dominate the reduction. However, further aggregation carries the risk of losing resolution and consequently the opportunities for detecting potential shifts in the outcome pool.

As this paper's analysis exposes internal perturbations and what they may represent (e.g., early warning signals), it omits study of the RHEA ABM's resilience to external shocks. However, a mechanism for an environmental disturbance is integrated and available in the model: a flood that may be set to occur at a pre-determined time step and can impact the model's housing market dynamics. With this mechanism, we can consider the standard definition of resilience in which a system may be characterized by its ability to function in the face an external perturbation, while maintaining its original configuration or adapting with a different configuration (Dragicevic, 2016; Folke, 2006). Thus, future investigation into how the MDS temporally reacts to a natural hazard event (flood) is feasible and would shed light on resilience in this coastal housing market model. Sudden irreducibility (i.e., lower correlation or higher RMSE) would then indicate that one or more of the outcomes from a subset of input parameters exhibit a reaction, or initial vulnerability, to the shock. Further departure could signify

exacerbation, if a trend of increasing irreducibility is observed, or a new equilibrium for those input parameter conditions inducing a resilience to the shock, if the trend stabilizes (i.e., plateaus). We observe the former pattern in the analysis of this paper, but the pattern is attributed to internal perturbations, since the external flood mechanism had not been engaged.

Still, what cannot be easily detected through the MDS would be the unlikely event of all input parameter sets' inducing similar resilience, or conversely vulnerability, in the face of the shock. In this case, not even a slight shift would be observed in the correlation trajectory, but at the same time, the model would be exhibiting a global reaction. By global, we mean certain outcomes across all parameter sets behaving similarly. This, in and of itself, is informative as it points to a common systemic behavior, but precise detection requires additional analytic tools to discern when this happens. One approach, similar to the distance method employed in this paper, would be to calculate inter-temporal distances (relative or absolute) between outcomes, e.g., Euclidean distances between each outcome (across all parameter sets) at time  $t$  and time  $t + 1$  or within a temporal window. The resultant vector at each time pairing – the length of which is the count of individual model outcomes considered in the MDS – can be either monitored individually or as an aggregate, say standard deviation assuming normalized distances, in order to detect massive deviations across time steps.

Given that our focus on both characterizing ABM outcomes via their reducibility and MDS algorithm performance for data reduction is limited to projections of two dimensions, a thorough examination might expand this dimensional testing range to include larger dimensional spaces, possibly up to one less than the full data space (i.e., number of outcome variables). There is likely to be a relationship between how much more information may be derived from larger projection spaces and the number of outcome variables employed in the reduction. This relationship is expected to be nonlinear, given that at some point, the number of reduced dimensions may closely mirror the outcome set itself, reducing the variability in the measures, hence their informativeness.

However, the limited number of dimensions for our analyses allowed us to uncover how the MDS algorithms can expose shifts in a model's behavior that depart from a stable trend, thereby exposing when the model might be less resilient, due to both internal perturbations and certain parameter settings. As mentioned above, this detection capability of MDSes is still limited because if all outcomes throughout all the tested parameters exhibit such departure in similar magnitudes, then the correlation measures would not detect the departure. While projections into a larger dimensional space (i.e., retrieving a larger coordinate space beyond two dimensions) would increase MDS accuracy, its capability for detecting these continuing departures – that could be signs of internal vulnerability – would diminish as the additional degrees of freedom would allow for greater alignment with original distance data even if one or several outcomes markedly deviate from a trend. That is, the more dimensions employed in dimension reduction, the less likely it would be for radical or gradual departures to be detected.

A more complete survey of the routines' sensitivities would also include sampling from several parametric distributional sources of data with varying levels of noise. Similarly, both the reducibility and congruence (to parameters) is dependent on the breadth of the parameter and outcome space (i.e., number of input parameters and outcomes employed in the reduction and congruence analysis). A fuller analysis should consider the sensitivity of the characterizations and algorithms' performance to the set variables (size and selection) and their interdependencies. The MDS routines also reveal aberrations in the both types of reducibility such as the sharp spikes and dips that warrant further investigation. Still, the analysis of this paper has helped us identify the outcome regimes of volatility in the model outcomes and lead us to rethink the level of the model complexity and redesign some

of its crucial components – in particular a reduction of dimensionality in the adaptive hedonic mechanism (de Koning et al., 2018) – and also redesign experimental procedures to focus on areas of relative equilibrium as confirmed by the MDS (de Koning et al., 2017). Identifying the triggers behind volatility then becomes the next investigative exercise. A more comparative approach comprising an omnibus of reductions to multiple sets of dimensions (i.e., 2 dimensions vs. 3 vs. 4, etc.) would help in identifying these triggers.

The RHEA ABM is distinct in that its initial states (e.g., housing prices) are derived from empirical data and are thus initially identical every simulation run. Many ABMs however do not exhibit this feature, so how reducibility will manifest when initial states can vary remains unknown. Still, the fixed initial states of this model offers one level of parsimony to our analysis. That is, we know the model's reducibility patterns under fixed states and can proceed to explore and compare against additional complexity derived from stochastic initial states.

Also, several of the outcomes in this paper are aggregated (average) measures and deemed appropriate given prior research on this model. Deeper exploration into using MDS to characterize ABM outcomes could operate at a more granular level. For example, in the RHEA ABM, the properties are fixed geographic locations, the selling prices of which can serve as separate outcomes. However, one caveat is that the outcome space will become exceedingly vast, and so dimension reduction would require significant computing resources. For practical purposes, we might instead consider incremental increases to granularity (e.g., slightly more granular aggregations than the highest levels), to see if their results deviate from the level of granularity employed in this paper. Furthermore, using MDS on highly granular outcomes rooted in changing populations (such as agents entering and leaving the ABM) may prove difficult as the pool of outcomes will vary significantly between time steps, possibly rendering any data reduction exercise uninformative.

Similarly, the choice of which input and outcome variables to include in the MDS analysis as well as the outcomes' comparison to model controls is subject to further discussion. While our selection was largely guided by previous work that points to input and outputs that are relevant to the aims of the RHEA ABM (Filatova, 2015) that serve to improve our understanding of its housing market as well as detection of regime shifts (Filatova et al., 2015), additional sensitivity tests using different input and outcome sets would allow one to better understand

## Appendix A. Description of the RHEA agent-based model

The outputs analyzed in this paper are drawn from an agent-based computational economics model of a spatially explicit empirical housing market. The model is titled *Risks and Hedonics in an Empirical Agent-Based Land-Market*, or RHEA, for short. Its development spans several publications, with its introduction, description, and experimental analysis appearing in Filatova (2015) and earlier developments in Filatova et al. (2011). The RHEA model simulates a bilateral, heterogeneous housing market in an empirical landscape. Buyers search for residential properties in the seaside town (Beaufort, North Carolina, USA) where both coastal amenities and environmental risks of flooding are spatially correlated. A realtor agent serves as a mediating agent that learns about the current market trend and willingness to pay for various spatial attributes of properties (Filatova, 2015). At each time step, sellers of the properties advertise their ask prices while buyers select and offer bids on properties. Then, the two groups engage in dyadic (pair-wise) negotiation which may or may not result in a successful transaction (i.e., trade).

The ask prices are primarily market-driven: each seller (1) consults with a realtor on the appropriate price given the current trends as estimated by a hedonic analysis of the recent simulated transactions and (2) adjusts the ask price if a property remains too long on a market. Buyers bid on the single property that brings them maximum utility and is affordable for their budgets. A buyer's budget constraints include their income, preference for amenities, a necessity to pay insurance premiums for flood-prone properties, and the possibility to activate an annual income growth. Spatial patterns of price dynamics and intensity of trade for particular types of properties are the emergent outputs of the model. When studying them under various parameter settings, we noticed that relative market power of buyers and sellers plays a role. The explanation is twofold. Firstly, a parcel that is very attractive will most likely receive several bid offers, out of which its seller chooses the highest, driving prices for most desirable properties up. Secondly, sellers of the properties that are less desirable may receive only one or even no bid offers, which can result in their selling at a lower price than initially planned or reducing their ask prices after a number of unsuccessful trades. Thus, excess demand drives prices up while excess supply pushes them down.

which variables actually drive reducibility for this or any other ABM.

This investigation also achieves a secondary goal. The use of multiple MDS routines to assess reducibility of this ABM's outcomes also exposes those routines' performance or accuracy. This paper thus addresses the question of which algorithm (among the ones surveyed) a researcher should employ. The facile answer is that it depends. The canonical algorithm, CMDS, is the most expedient yet the least accurate for all correlations and RMSE. How impactful this trade-off affects algorithm choice will depend on additional factors such as the volume of the researcher's data, which we discuss further in the limitations section of the paper. With the tested data, this trade-off was such that it would more beneficial to eschew CMDS in favor of the more accurate and complex methods.

On the opposite end of the cost-benefit spectrum lies the ISO algorithm. While this algorithm performs consistently well across all the accuracy measures, this benefit is muted by a severe cost in run time (see Appendix C), and thus its attractiveness as the algorithm of choice is relegated to the middle of the pack. Thus, one of NMDS routines appear optimal. Finally, if reduction of error (RMSE) is the primary objective, then SAM would be the best choice as its average performance exceeds all the other routines. The high correlative accuracies may be suitable for visualization and other similar purposes, but consideration of RMSE is more relevant for numerical accuracy.

Finally, the MDSes and dimension reduction in general are constantly undergoing improvements, so it would behoove us to expand the comparative analysis to include these advancements. Some of this work includes further development of the stress function in SAM (Sun et al., 2012) and approximations of CMDS under sparse conditions (Brandes and Pich, 2007). While these methods appear at times inferior to the other algorithms, their apparent ability to serve as an early-warning signal for systemic shifts warrants their further use and investigation.

## Acknowledgements

This material is based on work supported by Nederlandse Organisatie voor Wetenschappelijk Onderzoek DID MIRACLE (640-006-012), NWO VENI grant (451-11-033), and EU FP7 Ideas: European Research Council COMPLEX (308601). We also thank the anonymous reviewers for their detailed critiques and suggestions.

## Appendix B. Descriptions of input parameters and outcome variables

**Table B1**  
Input parameter descriptions.

Input Parameter	Description
<code>fraction_on_sale</code>	Mean proportion of properties initially on sale
<code>sd_fraction_on_sale</code>	The Gaussian standard deviation of proportion of properties, for random sampling
<code>new buyer coef.</code>	Rate at which new buyers enter the market
<code>prefAlfa</code>	Household preference for a housing good over a composite good.
<code>prefGamma</code>	Mean for household preference for coastal amenities
<code>Gsd</code>	Standard deviation for <code>prefGamma</code>
<code>delta coef.</code>	The acceptable difference between bid and ask prices for a trader during price negotiation, updated the longer a trader stays in the market
<code>loss coef.</code>	Proportion of property value loss due to flood
<code>refused die crit.</code>	Number of time steps of unsuccessful bids before buyer leaves the market
<code>refused price crit.</code>	Number of time steps of seller's property's not being sold before seller takes property off the market
<code>Insurance</code>	Indicator for availability of flood insurance for buyers

**Table B2**  
Input parameter notation and sampling ranges.

Parameter	Abbrv	Notation		Distr	Range	Default
<code>fraction_on_sale</code>	<code>fos</code>	$\mu(\text{Pr}\{\text{sale}\})$	~	Uniform	(0.05,0.60)	0.2
<code>sd_fraction_on_sale</code>	<code>sfos</code>	$\sigma(\text{Pr}\{\text{sale}\})$	~	Uniform	(0.005,0.10)	0.01
<code>new buyer coef.</code>	<code>nBC</code>	$\kappa_{\text{buyer}}$	~	Uniform	(0.5,1.0)	0.7
<code>prefAlfa</code>	<code>pA</code>	$\alpha$	~	Uniform	(0.4,0.6)	0.4
<code>prefGamma</code>	<code>pG</code>	$\gamma$	~	Uniform	(0.4,0.8)	0.5
<code>Gsd</code>	<code>Gsd</code>	$\sigma(\gamma)$	~	Uniform	(0.005,0.15)	0.05
<code>delta coef.</code>	<code>dC</code>	$\delta$	~	Uniform	(1.1,2.0)	1.5
<code>loss coef.</code>	<code>L</code>	$L$	~	Uniform	(0.01,1.0)	0.15
<code>refused die crit.</code>	<code>rDC</code>	$r_D$	~	[Uniform]	{2, ...,8}	4
<code>refused price crit.</code>	<code>rPC</code>	$r_p$	~	[Uniform]	{0, 1, 2}	1
<code>Insurance</code>	<code>Ins</code>	$I$	~	Binomial	{0, 1}	0

**Table B3**  
Outcome variable descriptions.

Outcome variable	Description
<code>totalPV</code>	Total market value of all residential properties
<code>avRent</code>	Average of residential property prices
<code>avUtil</code>	Average utility of all property owners
<code>avPriceFP0</code>	Average price of properties in the safe zone
<code>avPriceFP100</code>	Average price of flood-prone properties in the 1:100 years flood plain
<code>avPriceFP500</code>	Average price of flood-prone properties in the 1:500 years flood plain
<code>avPriceCoastFront</code>	Average price of coastal front properties
<code>NOFTrades</code>	Number of trades (sales) per round
<code>nRefusedSellers</code>	Number of sellers who were unsuccessful at the end of a time step
<code>nOfSellersLeft</code>	Number of sellers who left the city
<code>nOfSellersOffTr</code>	Number of sellers who left the market due to consecutive unsuccessful trades
<code>nOfBuyersLeft</code>	Number of buyers who left the city
<code>nNewSellers</code>	Number of new sellers entering the market at the beginning of a time step
<code>nOldSellers</code>	Number of sellers from the previous round
<code>nTotalSellers</code>	Number of total sellers (old and new)
<code>nNewBuyersOS</code>	Number of new buyers who were sellers in the previous step
<code>nNewBuyersNC</code>	Number of newcomer buyers
<code>nOldBuyers</code>	Number of buyers from the previous round
<code>nTotalBuyers</code>	Total number of buyers

**Table B4**  
Summary statistics of outcome variables.

	Min.	Median	Mean	Max.
totalPV (\$M)	201.7	1339.0	1728.0	542200.0
avRent (\$K)	1.0	6.3	8.2	2567.0
avPriceFP0 (\$K)	61.7	387.9	508.7	160800.0
avPriceFP100 (\$K)	5.6	442.9	565.9	162300.0
avPriceFP500 (\$K)	3.8	290.5	368.4	130400.0
avPriceCoastFront (\$K)	10.2	951.9	1232.0	170000.0
NOFTrades (K)	0.0	0.5	0.5	1.2
nRefusedSellers	0.0	335.0	450.0	2642.0
nOfSellersLeft	0.0	332.0	332.3	835.0
nOfSellersOffTr	0.0	88.0	104.5	705.0
nOfBuyersLeft	0.0	63.0	88.4	7456.0
nNewSellers	0.0	584.0	582.6	1702.0
nOldSellers	0.0	796.0	893.2	2772.0
nTotalSellers	0.0	1320.0	1371.0	3369.0
nNewBuyersOS	0.0	142.0	142.4	367.0
nNewBuyersNC	0.0	431.0	436.3	1466.0
nOldBuyers	0.0	799.0	1247.0	18050.0
nTotalBuyers	0.0	1316.0	1737.0	19240.0

### Appendix C. Run times of MDS algorithms

In Fig. C.5, we explore an additional performance metric: the run times of the routines. Due to the vagaries of computational processing, run times are neither exact nor as precise as algorithmic complexity. Still, they can offer a general indication of performance.

The y-axis is on a logarithmic scale, thus the linear increase in the plot maps to an exponential increase in the real run time. The run times expose both implementation idiosyncrasies as well as algorithmic stabilities. We first notice that ISO and NMDS hybrid run times are severely worse than other routines. Given that their accuracies are comparable or worse than the other NMDS variants tested, one should consider avoiding them altogether. Also, the SAM run times exhibits severe variance, which again highlights its instability. The linear NMDS routine appears to be most efficient, considering both its run time and accuracy over CMDS (refer to Fig. 2).

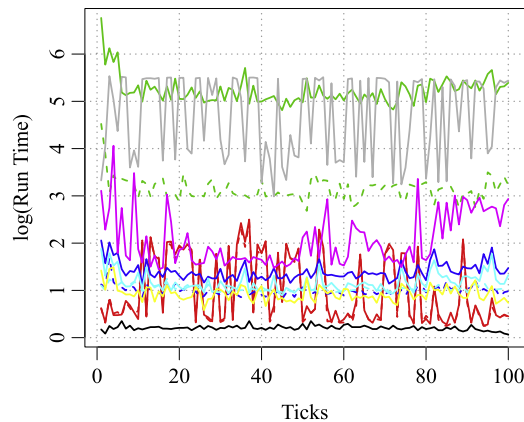


**Fig. C1.** Run times across time steps. (For interpretation of the references to color in this figure legend, the reader is referred to the web version of this article.)

**Table C1**  
Ranked run times.

Rank	MDS	Code	Average Run Time
1	classical	CMDS	1.2
2	linear	NMDS	2.6
3	global	NMDS	3.3
4	global w/scaling	NMDS	3.4
5	Sammon	SAM	3.6
6	local	NMDS	9.5
7	hybrid	NMDS	149.4
8	Kruskal	ISO	183.5

Run times are in seconds

## References

- Banda, J., Angryk, R., Martens, P., 2012. Quantitative comparison of linear and non-linear dimensionality reduction techniques for solar image archives. Florida Artificial Intelligence Research Society Conference.
- Bin, O., Kruse, J.B., Landry, C.E., 2008. Flood hazards, insurance rates, and amenities: evidence from the coastal housing market. *J. Risk Insurance* 75 (1), 63–82.
- Brandes, U., Pich, C., 2007. Eigensolver methods for progressive multidimensional scaling of large data. In: Kaufmann, M., Wagner, D. (Eds.), *Graph Drawing. Lecture Notes in Computer Science* 4372. Springer Berlin Heidelberg, pp. 42–53. [https://doi.org/10.1007/978-3-540-70904-6\\_6](https://doi.org/10.1007/978-3-540-70904-6_6).
- Brede, M., Boschetti, F., McDonald, D., 2008. Strategies for resource exploitation. *Ecol. Complexity* 5, 22–29.
- ten Broeke, G., van Voorn, G., Ligtenberg, A., 2016. Which sensitivity analysis method should i use for my agent-based model? *J. Artif. Soc. Social Simul.* 19 (1), 5. <https://doi.org/10.18564/jasss.2857>.
- ten Broeke, G., van Voorn, G., Ligtenberg, A., Molenaar, J., 2017. Resilience through adaptation. *PLoS ONE* 12 (2), e0171833. <https://doi.org/10.1371/journal.pone.0171833>.
- Callahan, R.J., 2005. Modeling the exchange of AIDS prevention and treatment strategies in Hong Kong. In: Terano, T., Kita, H., Kaneda, T., Arai, K., Deguchi, H. (Eds.), *Agent-Based Simulation: From Modeling Methodologies to Real-World Applications. Agent-Based Social Systems 1*. Springer Tokyo, pp. 26–36. [https://doi.org/10.1007/4-431-26925-8\\_3](https://doi.org/10.1007/4-431-26925-8_3).
- Carabine, E.A., Wainwright, J., Twyman, C., 2014. Narratives of a drought: exploring resilience in Kenya's drylands. In: Kamiński, B., Koloch, G. (Eds.), *Advances in Social Simulation: Proceedings of the 9th Conference of the European Social Simulation Association*. Springer Berlin Heidelberg, Berlin, Heidelberg, pp. 307–317. [https://doi.org/10.1007/978-3-642-39829-2\\_27](https://doi.org/10.1007/978-3-642-39829-2_27).
- Chok, N.S., 2008. Pearson's versus Spearman's and Kendall's correlation coefficients for continuous data. University of Pittsburgh.
- Clarke, K., 1993. Non-parametric multivariate analyses of change in community structure. *Aus. J. Ecol.* 18, 117–143.
- Clarke, K., Gorley, R., 2015. *PRIMER v7: user manual/tutorial. PRIMER-E*. Plymouth.
- Crouser, R.J., Kee, D.E., Jeong, D.H., Chang, R., 2012. Two visualization tools for analyzing agent-based simulations in political science. *Comput. Graph. Appl., IEEE* 32 (1), 67–77.
- Cunze, S., Tackenberg, O., 2015. Decomposition of the maximum entropy niche function—a step beyond modelling species distribution. *Environ. Modell. Software* 72, 250–260.
- Dragicevic, A.Z., 2016. From robustness to resilience: a network price identity approach. *Ecol. Complexity* 28, 47–53.
- Evans, A., Heppenstall, A., Birkin, M., 2013. Understanding simulation results. In: Edmonds, B., Meyer, R. (Eds.), *Simulating Social Complexity*. Springer Berlin Heidelberg, pp. 173–195. [https://doi.org/10.1007/978-3-540-93813-2\\_9](https://doi.org/10.1007/978-3-540-93813-2_9).
- Faith, D., Minchin, P., Belbin, L., 1987. Compositional dissimilarity as a robust measure of ecological distance. *Vegetatio* 69, 57–68.
- Fasham, M., 1977. A comparison of nonmetric multidimensional scaling, principal components and reciprocal averaging for the ordination of simulated coenoclines, and coenoplanes. *Ecology* 551–561.
- Filatova, T., 2015. Empirical agent-based land market: integrating adaptive economic behavior in urban land-use models. *Comput. Environ. Urban Syst.* 54, 397–413.
- Filatova, T., Lee, J.-S., Naimi, B., 2015. Housing markets and economic choices under uncertainty: Exploring non-linear market dynamics in a spatial agent-based model. 20th Annual Workshop on the Economic Science with Heterogeneous Interacting Agents (WEHIA).
- Filatova, T., Parker, D.C., van der Veen, A., 2011. The implications of skewed risk perception for a dutch coastal land market: insights from an agent-based computational economics model. *Agricult. Resour. Econ. Rev.* 40 (3), 405–423.
- Filatova, T., Verburg, P., Parker, D., Stannard, C., 2013. Spatial agent-based models for socio-ecological systems: challenges and prospects. *Environ. Modell. Software* 45, 1–7.
- Folke, C., 2006. Resilience: the emergence of a perspective for social-ecological systems analyses. *Global Environ. Change* 16 (3), 253–267.
- Garces, M., Alcorn, B., 2012. Nesting a data-driven agent-based model within a theoretical framework. *Procedia Comput. Sci.* (Special Issue on the International Workshop on Advances in Computational Social Science, 000–000).
- Giraudel, J., Lek, S., 2001. A comparison of self-organizing map algorithm and some conventional statistical methods for ecological community ordination. *Ecol. Modell.* 146 (1), 329–339.
- Giuliani, M., Galelli, S., Soncini-Sessa, R., 2014. A dimensionality reduction approach for many-objective markov decision processes: application to a water reservoir operation problem. *Environ. Modell. Software* 57, 101–114.
- Gower, J.C., 1966. Some distance properties of latent root and vector methods used in multivariate analysis. *Biometrika* 53, 325–328.
- Grimm, V., Railsback, S., 2005. *Individual-Based Modeling and Ecology*. Princeton University Press, Princeton, NJ.
- Guisan, A., Zimmermann, N.E., 2000. Predictive habitat distribution models in ecology. *Ecol. Modell.* 135 (2), 147–186.
- Gutierrez, E., Lozano, S., Moreira, M.T., Feijoo, G., 2010. Assessing relationships among life-cycle environmental impacts with dimension reduction techniques. *J. Environ. Manage.* 91 (4), 1002–1011.
- Hui, F.K., Taskinen, S., Pledger, S., Foster, S.D., Warton, D.I., 2015. Model-based approaches to unconstrained ordination. *Methods Ecol. Evol.* 6 (4), 399–411.
- Jayyousi, T.W., Reynolds, R.G., 2012. Bringing to life an ancient urban center at Monte Albán, Mexico: exploiting the synergy between the micro, meso, and macro levels in a complex system. *Proceedings of the International Conference on Brain-Mind*. Brain Mind Institute.
- Kaplan, M., 2011. Agent-based modeling of land-use changes and vulnerability assessment in a coupled socio-ecological system in the coastal zone of Sri Lanka. ULB Bonn Ph.D. Thesis.
- Karsai, I., Roland, B., Kampis, G., 2016. The effect of fire on an abstract forest ecosystem: an agent based study. *Ecol. Complex.* 28, 12–23.
- Kendall, M., 1938. A new measure of rank correlation. *Biometrika* 30 (1–2), 81–89.
- Kenkel, N.C., Orlóci, L., 1986. Applying metric and nonmetric multidimensional scaling to ecological studies: some new results. *Ecology* 67 (4), 919–928.
- Kirt, T., Vainik, E., 2007. Comparison of the methods of self-organizing maps and multidimensional scaling in analysis of Estonian emotion concepts. In: Nivre, J., Kaalep, H.-J., Muisnec, K., Koit, M. (Eds.), *Proceedings of the 16th Nordic Conference of Computational Linguistics*. University of Tartu, Tartu, Estonia, pp. 113–120.
- de Koning, K., Filatova, T., Bin, O., 2017. Bridging the gap between revealed and stated preferences in flood-prone housing markets. *Ecol. Econ.* 136, 1–13.
- de Koning, K., Filatova, T., Bin, O., 2018. Improved methods for predicting property prices in hazard prone dynamic markets. *Environ. Resour. Econ.* 1–17.
- Lade, S.J., Gross, T., 2012. Early warning signals for critical transitions: a generalized modeling approach. *PLoS Comput. Biol.* 8 (2), e1002360.
- Lee, G., Rodriguez, C., Madabhushi, A., 2007. An empirical comparison of dimensionality reduction methods for classifying gene and protein expression datasets. *Bioinformatics Research and Applications*. Springer, pp. 170–181.
- Lee, J.-S., Filatova, T., Ligmann-Zielinska, A., Hassani-Mahmooei, B., Stonedahl, F., Lorscheid, I., Voinov, A., Polhill, J.G., Sun, Z., Parker, D.C., 2015. The complexities of agent-based modeling output analysis. *J. Artif. Soc. Social Simul.* 18 (4), 4. <https://doi.org/10.18564/jasss.2897>.
- van der Maaten, L.J., Postma, E.O., van den Herik, H.J., 2009. Dimensionality reduction: a comparative review. *J. Mach. Learn. Res.* 10 (1–41), 66–71.
- Manson, S.M., Sun, S., Bonsal, D., 2012. Agent-based modeling and complexity. In: Heppenstall, A.J., Crooks, A.T., See, L.M., Batty, M. (Eds.), *Agent-Based Models of Geographical Systems*. Springer Netherlands, Dordrecht, pp. 125–139. [https://doi.org/10.1007/978-90-481-8927-4\\_7](https://doi.org/10.1007/978-90-481-8927-4_7).
- Mantel, N., 1967. The detection of disease clustering and a generalized regression approach. *Cancer Res.* 27 (2), 209–220.
- McCune, B., Mefford, M.J., 1999. *PC-ORD: Multivariate analysis of ecological data*. MjM Software Design.
- Minchin, P., 1987. An evaluation of relative robustness of techniques for ecological ordinations. *Vegetatio* 69, 89–107.
- Murota, M., Inoue, J.-I., 2014. Characterizing financial crisis by means of the three states random field ising model. *Econophysics of Agent-Based Models*. Springer, pp. 83–98.
- Nakada, T., Takadama, K., Watanabe, S., 2011. Bayesian analysis method of time series data in greenhouse gas emissions trading market. *Agent-Based Approaches in Economic and Social Complex Systems VI*. Springer, pp. 147–159.
- Oksanen, J., Blanchet, F. G., Kindt, R., Legendre, P., Minchin, P. R., O'Hara, R. B., Simpson, G. L., Solymos, P., Stevens, M. H. H., Wagner, H., 2016. *vegan: Community Ecology Package*. R package version 2.3-3.
- Pearson, K., 1895. Notes on regression and inheritance in the case of two parents. *Proc. R. Soc. Lond.* 58, 240–242.
- Prentice, I., 1977. Non-metric ordination methods in ecology. *J. Ecol.* 85–94.
- Qian, S.S., King, R.S., Richardson, C.J., 2003. Two statistical methods for the detection of environmental thresholds. *Ecol. Modell.* 166 (1), 87–97.
- Ratzé, C., Gillet, F., Müller, J.-P., Stoffel, K., 2007. Simulation modelling of ecological hierarchies in constructive dynamical systems. *Ecol. Complexity* 4, 13–25.
- Sammon, J.W., 1969. A non-linear mapping for data structure analysis. *IEEE Trans. Comput.* C-18, 401–409.
- Scheffer, M., Bascompte, J., Brock, W.A., Brovkin, V., Carpenter, S.R., Dakos, V., Held, H., Van Nes, E.H., Rietkerk, M., Sugihara, G., 2009. Early-warning signals for critical transitions. *Nature* 461 (7260), 53.
- Schroeder, M., Noy, P., 2001. Multi-agent visualisation based on multivariate data. *Proceedings of the fifth international conference on Autonomous agents*. ACM, pp. 85–91.
- SPARCS, 2018. What are early warning signals? <http://www.early-warning-signals.org/theory/what-are-early-warning-signals>. Synergy Program for Analyzing Resilience and Critical Transitions.
- Sudheer, K., Lakshmi, G., Chaubey, I., 2011. Application of a pseudo simulator to evaluate the sensitivity of parameters in complex watershed models. *Environ. Modell. Software* 26 (2), 135–143.
- Sun, J., Fyfe, C., Crowe, M., 2012. Extending Sammon mapping with Bregman divergences. *Inf. Sci.* 187, 72–92. <https://doi.org/10.1016/j.ins.2011.10.013>.
- Thiele, J.C., Grimm, V., 2010. NetLogo meets R: linking agent-based models with a toolbox for their analysis. *Environ. Modell. Software* 25 (8), 972–974.
- Torgerson, W.S., 1958. *Theory and Methods of Scaling*. Wiley, New York.
- Turati, P., Pedroni, N., Zio, E., 2016. Dimensionality reduction of the resilience model of a critical infrastructure network by means of elementary effects sensitivity analysis. *Risk, Reliability and Safety: Innovating Theory and Practice: Proceedings of European Safety and Reliability Conference (ESREL) 2016*. Glasgow, United Kingdom, pp. 2797–2804.
- Venables, W.N., Ripley, B.D., 2002. *Modern Applied Statistics with S*, Fourth. Springer, New York. ISBN 0-387-95457-0
- Walker, B., Salt, D., 2006. *Resilience Thinking: Sustaining Ecosystems and People in a Changing World*. Island Press, Washington, D.C.
- Zia, A., Bombles, A., Schroth, A.W., Koliba, C., Isles, P.D.F., Tsai, Y., Mohammed, I.N., Bucini, G., Clemins, P.J., Turnbull, S., Rodgers, M., Hamed, A., Beckage, B., Winter, J., Adair, C., Galford, G.L., Rizzo, D., Houten, J.V., 2016. Coupled impacts of climate and land use change across a riverlake continuum: insights from an integrated assessment model of lake champlains missisquoi basin, 20002040. *Environ. Res. Lett.* 11 (11), 114026.